ELSEVIER

Chemical Engineering Journal 68 (1997) 165–172

Chemical Engineering Journal

# Modelling and simulation of extraction of oligomer from granular polymers

Z. Chen [a], J. Prüss [b], D. Meier [a], H.-J. Warnecke [a]

[a] *Chemical Engineering, University of Paderborn, 33098 Paderborn, Germany*

[b] *FB Mathematik and Informatik, Martin Luther University, 06099 Halle, Germany*

Received 17 December 1996; revised 11 July 1997; accepted 14 July 1997

**Abstract**

A mathematical model has been developed for the extraction of oligomers from granular polymers with solvent. The model accounts for effective diffusion of the oligomer in the polymer pearls, axial dispersion of the pellets and liquid phase and distribution equilibrium at the interface. The results of numerical simulations of the model are consistent with experimental data. The influence of the physico-chemical parameters on the oligomer concentration in the pellets is shown in terms of a sensitivity analysis. The model can be used for analysis and design calculation of extraction of oligomers either in batch or continuous processes. © 1997 Elsevier Science S.A.

*Keywords:* Granular polymers; Oligomer extraction; Modelling

## 1. Introduction

Polymer products often contain low molecular weight oligomers that may deteriorate the product characteristics. The removal of oligomers from granular polymers is therefore a problem frequently encountered in the production of pure polymers. There are a number of studies in the literature that describe extraction techniques for removing oligomers from polymers, which are already in use. BASF Company reported their work on the extraction of oligomers from polyamide using hot water [1]. US Patent 4,306,058 [2] described the removal of cyclic oligomers from polyoxyalkylene using supercritical propylene. Barry et al. [3] discussed the upgrading of a silicone polymer, designated OV-17, used as a gas chromatography stationary phase. An interesting study of the extraction of oligomers from polyamide by methanol has been presented by Sridhar and Hartig [4]. They employed a simple diffusion model to simulate extractor behaviour. In ref. [5], an axial dispersion model for a two stage extraction was discussed. One of the purposes of these investigations was the determination of the important parameters for the design, operation and optimization of plant performance. However, in spite of the large number of studies, such processes cannot be considered to be well understood.

The industrial process is carried out either by discontinuous or continuous extraction. For continuous operation, flow of polymer and solvent can be arranged in three ways: (1) cocurrent, (2) countercurrent, and (3) crosscurrent. In general, countercurrent operation gives higher efficiency. When the extracting solvent and raffinate solvent are immiscible, countercurrent operations are the method of extraction most commonly used. In this article investigations on discontinuous and continuous countercurrent extractions are described.

The model developed below is applied to extraction of oligomers from polyamide by methanol. The identified parameters are estimated from experiments by Sridhar and Hartig [4] using nonlinear regression (Marquardt's method). The behaviour of the extractor is then simulated numerically. As will be shown in this paper, the results of model predictions are in good agreement with experimental data.

## 2. Model description

To design an extractor, appropriate models for the system must be constructed that accurately describe the phenomena occurring within it. Besides diffusion through the pellet and liquid phases, the microscopic interfacial transport process and macroscopic hydrodynamic properties of the reactor are important. When intraparticle diffusion controls the mass transfer process, it is reasonable to begin with the description of mass transfer between a single spherical pellet and the surrounding solvent and then to extend the model to the whole extractor. The extraction process from a pellet may be described by the following stages in series: (1) volatile


*PII* S1385-8947(97)00079-X

organic components diffuse linearly from the interior to the outer surface of the pellet; (2) at the interfacial area the oligomer is transferred to the solvent; (3) product diffuses through a stationary film around the pellet into the bulk of liquid phase; (4) macroscopic transport of transferred component in the solvent and of the polymer pellets by convection and dispersion takes place. In stage (2), the thermodynamic equilibrium of the oligomer between the solid phase and the liquid phase plays a crucial role.

Mathematically, the overall extraction of the contaminant from the solid pellets can be described by a set of partial differential equations. The assumptions of the model are:

- The system is isothermal.
- The pellets are of a spherical shape and identical size.

### 2.1. Material balance for a semi-batch extractor

The differential material balance for a single pellet of radius $R$ in spherical coordinates is given by

$$\frac{\partial c(t,r)}{\partial t}=\frac{D}{r^2}\frac{\partial}{\partial r}\left[r^2\frac{\partial c(t,r)}{\partial r}\right] \quad t>0 \quad 0<r<R$$
$$\frac{\partial c(t,0)}{\partial r}=0 \qquad c(0,r)=c_0 \tag{1}$$

where $c(t,r)$ denotes the concentration of the oligomer in the pellet as a function of extraction time $t$ and radial coordinate $r$; $D$ is the diffusion coefficient of oligomer in the pellet phase.

The differential material balance for the interface liquid-side film is accordingly

$$\frac{\partial c(t,r)}{\partial t}=\frac{D_L}{r^2}\frac{\partial}{\partial r}\left[r^2\frac{\partial c(t,r)}{\partial r}\right] \qquad t>0 \qquad R<r<R+\delta$$
$$h[c(t,R-)]=c(t,R+) \qquad D\frac{\partial c(t,R-)}{\partial r}=D_L\frac{\partial c(t,R+)}{\partial r}$$
$$c(t,R+\delta)=c^b(t) \qquad c(0,r)=c_0 \tag{2}$$

where $D_L$ is the diffusion coefficient of oligomer in the bulk phase, $c^b(t)$ denotes the concentration of oligomer in the solvent, $\delta$ is the thickness of the interfacial film, and $h(c)$ the interfacial equilibrium relation for oligomer between the pellet phase and bulk phase.

The differential material balance for the bulk phase is

$$V_L\frac{\partial c^b(t)}{\partial t}=-A_L D_L\frac{\partial c(t,R+\delta)}{\partial r}-\dot{V}_L c^b(t) \quad c^b(0)=c_0^b=0 \tag{3}$$

where $A_L$ denotes the interfacial area, $V_L$ and $\dot{V}_L$ the solvent volume and solvent volumetric flow rate, respectively, and $c_0^b$ the initial concentration in solvent. Fig. 1 gives a schematic diagram of the extraction process in a well-mixed semi-batch extractor.

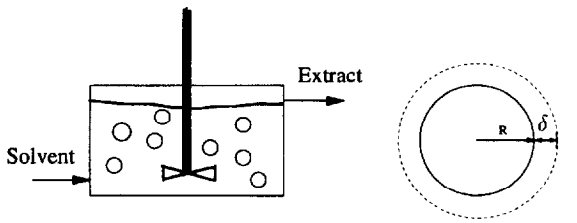


(a) A semibatch reactor (b) A polymer pellet

Fig. 1. A semi-batch unit and a polymer pellet.

Assuming that oligomer diffusion in the film is rapid, which means $\partial c(t,r)/\partial t\approx 0$, $R<r<R+\delta$, Eq. (2) can be solved for the concentration in the film:

$$c(t,r)=\frac{R(R+\delta)}{r\delta}\{h[c(t,R-)]-c^b(t)\}+\left(1+\frac{R}{\delta}\right)c^b(t)-\frac{R}{\delta}h[c(t,R-)] \quad R<r<R+\delta \tag{4}$$

This implies for the mass diffusion through the pellet surface,

$$D\frac{\partial c(t,R-)}{\partial r}=D_L\frac{\partial c(t,R+)}{\partial r}=\frac{D_L(R+\delta)}{R\delta}\{c^b(t)-h[c(t,R-)]\} \tag{5}$$

as well as for the bulk side,

$$D_l\frac{\partial c(t,R+\delta)}{\partial r}=\frac{D_L R}{\delta(R+\delta)}\{c^b(t)-h[c(t,R-)]\} \tag{6}$$

Scaling the radius $R$ to 1, the semi-batch model can be reduced to the following dimensionless equations:

$$\frac{\partial u(t,r)}{\partial t}=\frac{1}{\tau_D r^2}\frac{\partial}{\partial r}\left[r^2\frac{\partial u(t,r)}{\partial r}\right] \quad t>0 \quad 0<r<1$$
$$\frac{\partial u^b(t)}{\partial t}=-\frac{3\eta\gamma}{\tau_D}\{u^b(t)-H[u(t,1)]\}-\frac{u^b(t)}{\tau}$$
$$\frac{\partial u(t,1)}{\partial r}=\gamma\{u^b(t)-H[u(t,1)]\} \tag{7}$$
$$\frac{\partial u(t,0)}{\partial r}=0 \quad u(0,r)=1 \quad u^b(0)=0$$

The dimensionless variables are defined as follows:

$$u=\frac{c}{c_0} \quad u^b=\frac{c^b}{c_0} \quad \tau_D=\frac{R^2}{D}$$
$$\gamma=\frac{D_L}{D}\left(1+\frac{R}{\delta}\right) \quad \eta=\frac{V_p}{V_L} \quad \tau=V_L/\dot{V}_L \tag{8}$$

with

$$A_L=4\pi(R+\delta)^2 n \quad V_L=V_R-\frac{4\pi}{3}(R+\delta)^3 n$$
$$H(u)=h(c_0 u)/c_0 \tag{9}$$

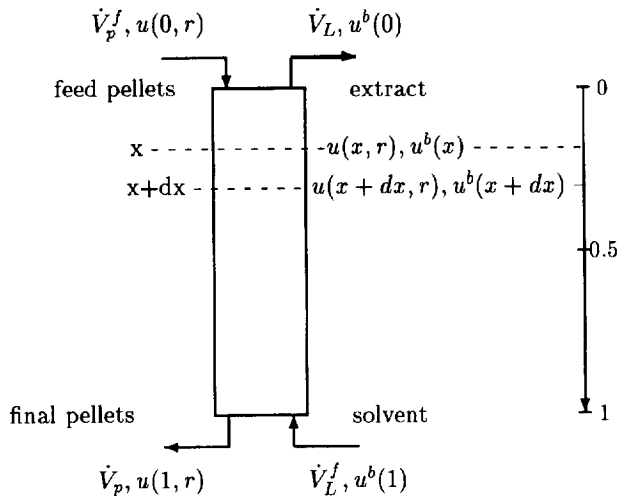


Fig. 2. Operating scheme of continuous countercurrent extraction.

where $n$ means the number of pellets and $V_R$ the extractor volume.

### 2.2. Material balance for a continuous countercurrent extractor in steady state

Fig. 2 shows the operating scheme of a continuous countercurrent extractor. Taking into account axial dispersion in a plug–flow model the differential equations for the concentration of oligomer in both phases are:

$$0=\frac{1}{Bo_p}\frac{\partial^2 u(x,r)}{\partial x^2}-\frac{\partial u(x,r)}{\partial x}+\frac{\sigma}{r^2}\frac{\partial}{\partial r}\left[r^2\frac{\partial u(x,r)}{\partial r}\right] \quad x\in[0,1] \quad r\in[0,1]$$

$$0=\frac{1}{Bo_L}\frac{\partial^2 u^b(x)}{\partial x^2}+\frac{\partial u^b(x)}{\partial x}-3\eta\gamma\rho\{u^b(x)-H[u(x,1)]\} \quad x\in[0,1] \tag{10}$$

with

$$Bo_j=lu_j/E_j \quad \tau_j=l/u_j \quad \sigma=\tau_p/\tau_D \quad \rho=\tau_L/\tau_D \quad j=p,L \tag{11}$$

where $Bo_j$ is the Bodenstein number, $E_j$ the dispersion coefficient, $\tau_j$ the residence time, $u_j$ the flow velocity of the phases, $j=p,L$, respectively, and $l$ means extractor length.

The associated boundary conditions formulated according to Danckwerts are:

$$\frac{1}{Bo_p}\frac{\partial u(0,r)}{\partial x}-u(0,r)=-1 \qquad \frac{\partial u(1,r)}{\partial x}=0$$

$$\frac{\partial u(x,1)}{\partial r}=\gamma\{u^b(x)-H[u(x,1)]\} \qquad \frac{\partial u(x,0)}{\partial r}=0 \tag{12}$$

$$\frac{1}{Bo_L}\frac{\partial u^b(1)}{\partial x}+u^b(1)=0 \qquad \frac{\partial u^b(0)}{\partial x}=0$$

The dimensionless model Eqs. (7)–(12) can be used for simulation of the above described extractor with appropriate parameter values. From the semi-batch Eqs. (7)–(9) one can identify important model parameters governing the dynamic behaviour of the system. $H$, $\gamma$ and $\tau_D$ are determined from experimental data. $Bo_p$ and $Bo_L$ can be estimated from the operating conditions of the reactor.

## 3. Numerical solution

The most commonly used technique to solve the system of Eq. (7) is the finite-difference method [6], but this method requires strict conditions for stability. In the linear case, the system can be solved analytically by Fourier transform [7,8], but this method cannot be applied to nonlinear systems. A finite-difference-differential algorithm is developed and used in the simulation of the semi-batch and the continuous processes. An outline will be presented here for the continuous system.

Eq. (10) is a system of elliptic partial differential equations and their boundary conditions are coupled by an ordinary differential equation. In this approach Eq. (10) is first reduced to a two-point boundary-value problem for $N$ ordinary differential equations by discretization in the radial variable $r$, with local error of order $N^{-2}=h^2$:

$$0=\frac{1}{Bo_p}\frac{\partial^2 u_0(x)}{\partial x^2}-\frac{\partial u_0(x)}{\partial x}+6N^2\sigma[u_1(x)-u_0(x)]$$

$$0=\frac{1}{Bo_p}\frac{\partial^2 u_i(x)}{\partial x^2}-\frac{\partial u_i(x)}{\partial x}+N^2\sigma\left[\left(1+\frac{1}{i}\right)u_{i+1}(x)+\left(1+\frac{1}{i}\right)u_{i-1}(x)-2u_i(x)\right] \quad i=1,\ldots,N-1$$

$$0=\frac{1}{Bo_p}\frac{\partial^2 u_N(x)}{\partial x^2}-\frac{\partial u_N(x)}{\partial x}+N^2\sigma\left[\frac{8u_{N-1}(x)-u_{N-2}(x)-7u_N(x)}{2}\right]+\sigma(2+3N)\gamma\{u_{N+1}(x)-H[u_N(x)]\}$$

$$0=\frac{1}{Bo_L}\frac{\partial^2 u_{N+1}(x)}{\partial x^2}+\frac{\partial u_{N+1}(x)}{\partial x}+3\eta\gamma\rho\{H[u_N(x)]-u_{N+1}(x)\} \tag{13}$$

The discretized boundary conditions become:

$$\frac{1}{Bo_p}\frac{\partial u_i(0)}{\partial x}-u_i(0)=-1 \qquad \frac{\partial u_i(1)}{\partial x}=0 \quad i=0,\ldots,N-1$$

$$\frac{1}{Bo_L}\frac{\partial u_{N+1}(1)}{\partial x}+u_{N+1}(1)=0 \qquad \frac{\partial u_{N+1}(0)}{\partial x}=0 \tag{14}$$

Here $u_0$ means concentration at the centre of the pellets, $u_N$ at the surface, and $u_{N+1}$ refers to the concentration of the solvent. Then, the solution of Eqs. (13) and (14) can be computed using a deferred correction technique and Newton iteration. The details of the algorithm and its advantages are described elsewhere [9,10].

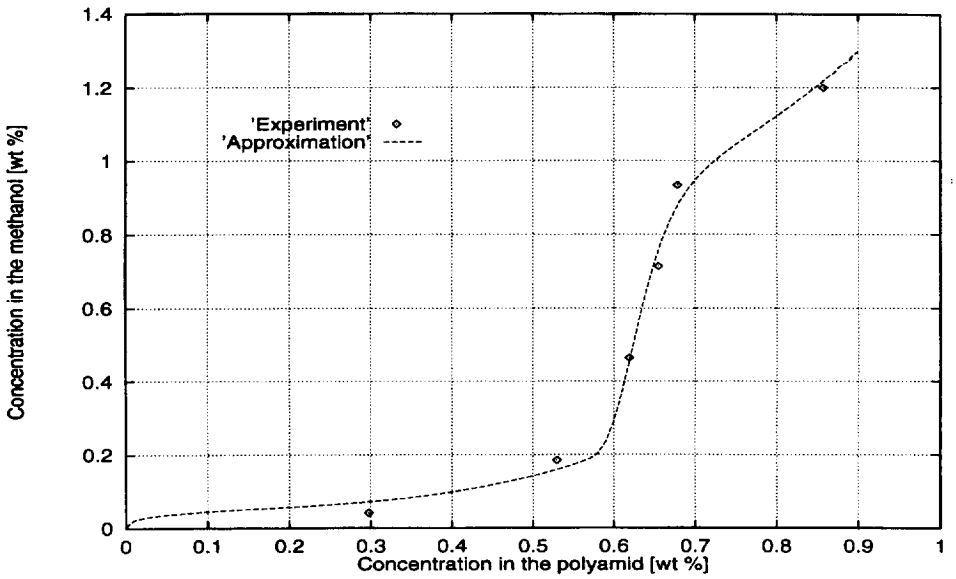


Fig. 3. Equilibrium distribution for the oligomer concentration between methanol and polyamid67C:\CEJ\3279\e at 338 K.

The mean concentration of the oligomer was computed at each length step as

$$\bar{u}(x) = \frac{4\pi}{4\pi/3}\int_0^1 u(x,r)r^2\,\mathrm{d}r = 3\int_0^1 u(x,r)r^2\,\mathrm{d}r$$

$$\approx h^3\left[\sum_{i=0}^{N-1} u_i(x)(1+3i+3i^2)\right] \qquad (15)$$

where $h=1/N$ means the discretization step size. This approximation is accurate up to order $h^2$.

## 4. Model application and discussion

In order to demonstrate the application of our model and computational algorithm, we consider the extraction of oligomer from polyamide-12 by methanol and discuss model prediction capability. The first task in the modelling of a specific system is to determine the appropriate system parameters. In fact, only the function $h(c)$ and the parameters $D$ and $\gamma$ have to be fitted to experimental data.

### *4.1. Parameter identification and batch-model simulation*

We begin with parameters for interfacial equilibrium relation $h(c)$. According to the data obtained by Sridhar and Hartig [4], a new correlation of the distribution of the oligomer concentration between the methanol and the polyamide was derived. It is given as follows:

$$h(c) = k_1 c^{0.3} + (c-k_1)^3 + k_2 \exp[k_3 \exp(k_4 c)] \qquad (16)$$

where $k_1$, $k_2$, $k_3$ and $k_4$ are experimental parameters, determined as follows: $k_1 = 0.08951$, $k_2 = 0.6811$, $k_3 = -3.140\times 10^9$ and $k_4 = -35.18$. Fig. 3 shows the equilibrium data and the curve fitting results.

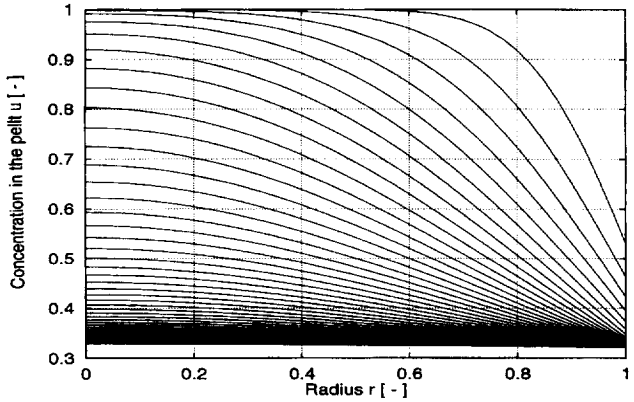


Fig. 4. Dimensionless concentration profiles of oligomer in a pellet. Concentration curves are spaced at 7 min intervals.

We now consider $D$ and $\gamma$, which are not available in the literature. These were assumed to be independent of concentration and were estimated according to the semi-batch model (Eqs. (7)–(9)) by fitting the extraction experimental data obtained by Sridhar and Hartig [4] under experimental conditions ($c_0 = 2$ wt.%, $R = 0.1$ cm, $T = 338$ K, $\eta = 0.5$, $\dot{V}_L = 0$ cm$^3$ and $V_R = 1000$ cm$^3$), yielding

$$D = 1.601\times 10^{-5}\ \mathrm{cm^2\ min^{-1}} \quad \gamma = 3.5$$

Fig. 4 shows the dimensionless concentration of the oligomer along the pellet radius at different extraction times, as obtained from Eq. (7) with the above parameters. Concentration curves are spaced at 7 min intervals of the contact time during the noncontinuous process. Concentration differences against the particle radius tend to decrease with extraction time. Surface concentration reaches much lower values than the initial one, confirming that mass transfer resistance is significantly lower than the internal one, however not negligible.

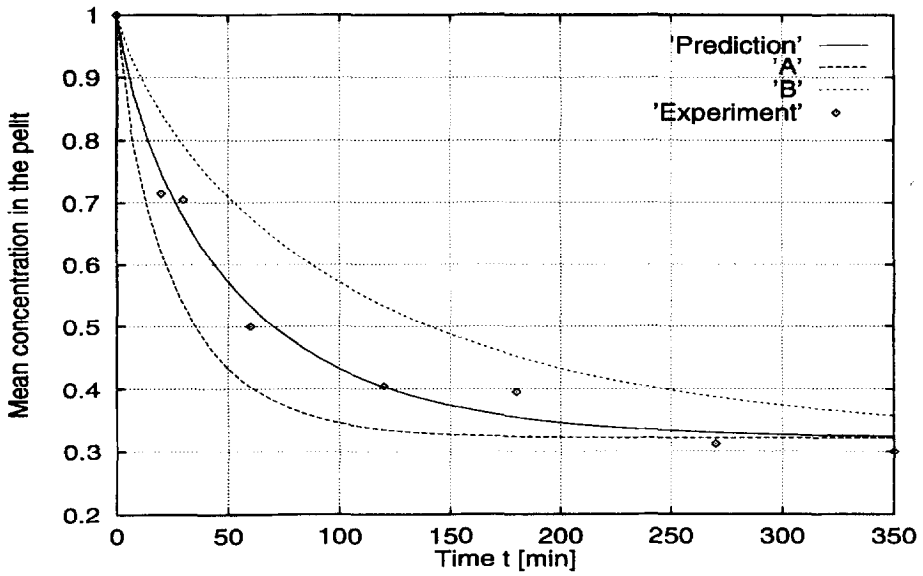


Fig. 5. Sensitivity analysis of diffusion parameter $D$ on the mean concentration of oligomer $\bar{u}(t)$ (A: $2D$; B: $0.5D$).

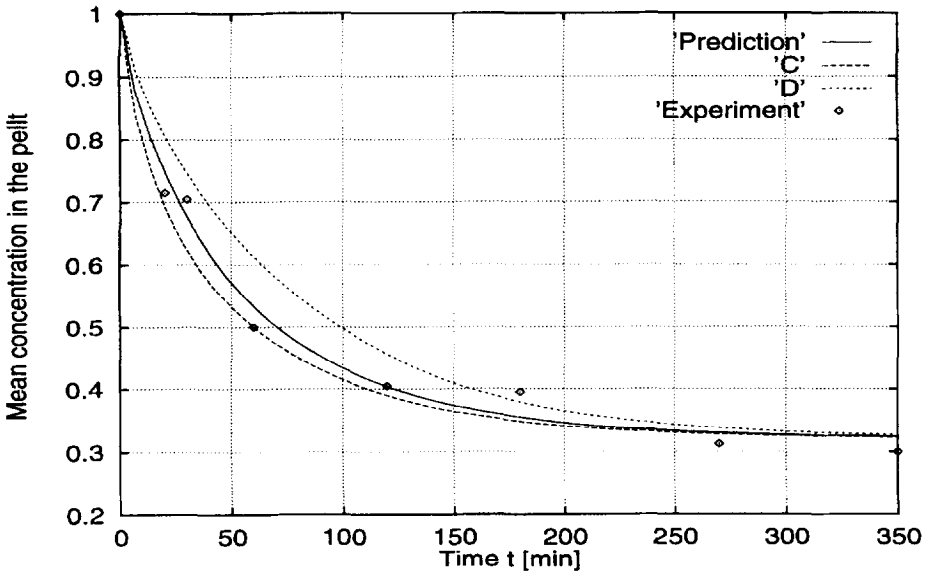


Fig. 6. Sensitivity analysis of resistance parameter $\gamma$ on the mean concentration of oligomer $\bar{u}(t)$ (C: $2\gamma$; D: $0.5\gamma$).

To determine the importance of the model parameters, the sensitivity of the model to the extraction parameters ($D$, $\gamma$ and $\eta$) was assessed by simulating the extraction profile. Fig. 5 shows the dimensionless mean concentration of the oligomer in the pellet phase as a function of time $t$. The prediction curve is for the optimum extraction parameters used for the simulation of the batch reactor experiment. Curve A is for a diffusion coefficient increased by a factor of 2 above the determined diffusivity, and curve B is for a diffusion coefficient decreased by a factor of 1/2 standard parameters. Curves C and D are for $\gamma$ and curves E and F for $\eta$ (Figs. 6 and 7 ) with the same variation factors as the diffusion coefficient in Fig. 5. The change in the values of $D$ or $\gamma$ produces a significant change in the middle portion, but only a small change in the tail of the extraction profile due to distribution equilibrium. As expected, the concentration of the oligomer in the pellet phase at the bottom end of the column decreases with increasing volume of solvent. The evaluated yields show a good fit for the batch extraction process. The multiple correlation parameter of the fit is larger than 0.99.

### 4.2. Model simulation of the countercurrent extractor

Having determined the batch model parameters, it is interesting to test the continuous model. The remaining parameters

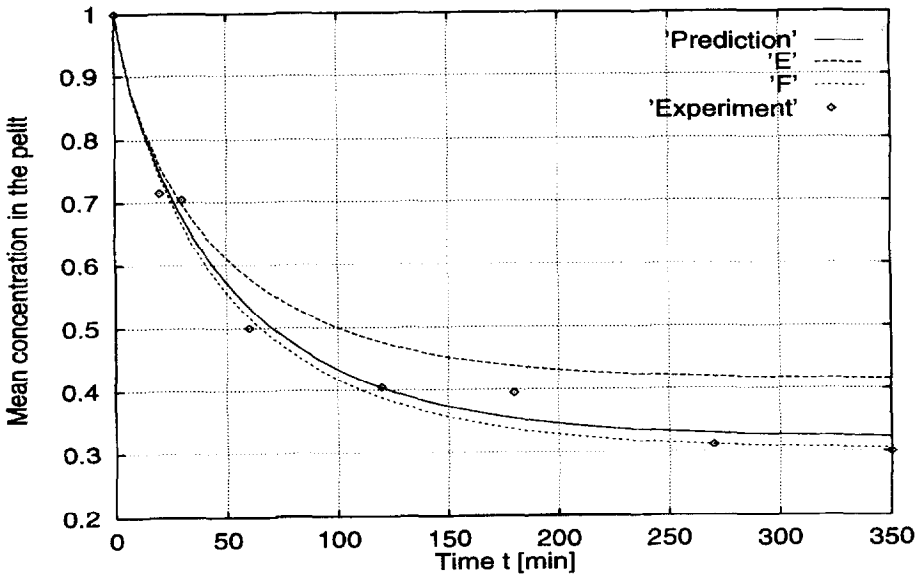


Fig. 7. Effect of the phase ratio $\eta$ on the mean concentration of oligomer $\bar{u}(t)$ (E: $2\eta$; F: $0.5\eta$).

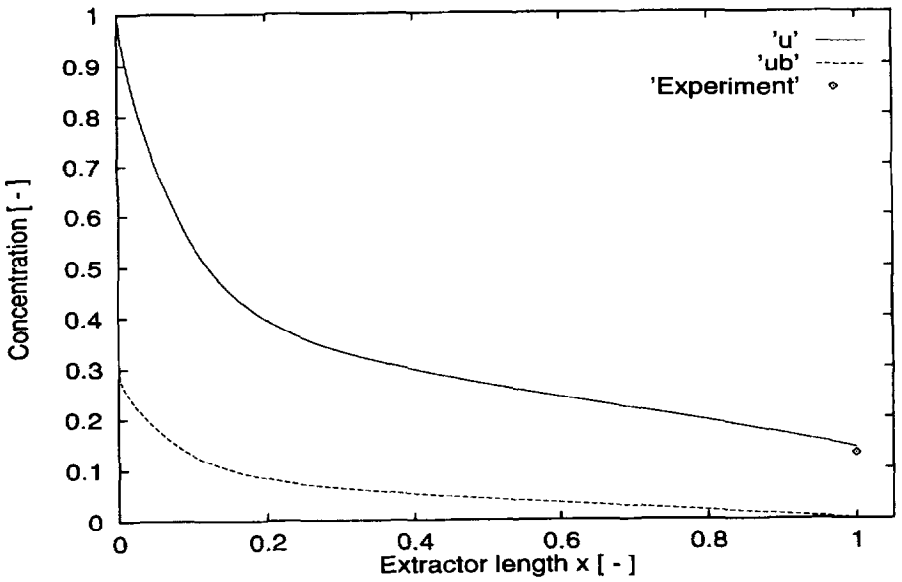


Fig. 8. Dependence of $\bar{u}(x)$ and $u^b(x)$ on $x$ ($Bo_p = 778$, $Bo_L = 41.7$).

$Bo_j$ are detected from experimental data obtained by Sridhar and Hartig [4] under the operating conditions of the countercurrent extraction process ($c_0 = 2$ wt.%, $R = 0.1$ cm, $\bar{V}_L/\bar{V}_p = 3$, $\tau_p = 600$ min, $l = 200$ cm, $d = 8$ cm and $T = 338$ K). The best fit of the data to the simulation results of the model obtained the following values: $Bo_p = 778$, $Bo_L = 41.7$. In Fig. 8 $\bar{u}$ and $\bar{u}^b$ are plotted versus $x$. This figure indicates that the model has a good agreement with the experimental data. The results may be represented in a three-dimensional plot such as that shown in Fig. 9.

For a real extraction system, the effect of backmixing on mass transfer is important. Fig. 10 demonstrates the influence of backmixing on $\bar{u}(1)$ in the terms of the $Bo_p$ and $Bo_L$ number, respectively. Decreasing backmixing, i.e. increasing the $Bo_j$ numbers, diminishes considerably the remaining content of oligomer in the pellets. At low Bo numbers (e.g.

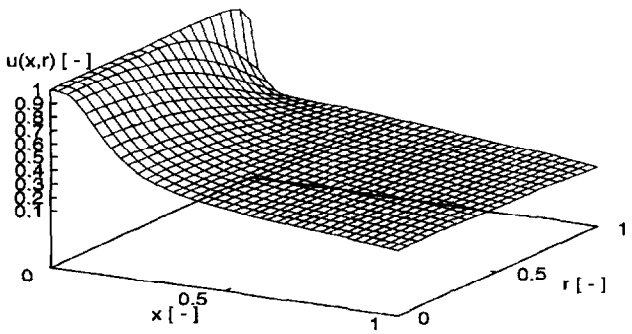


Fig. 9. Solution surfaces for the continuous model.

approximately less than 0.1) the concentration is relatively independent of the length of the extractor, and at the inlet of the extractor the initial concentration decreases instantaneously to exit concentration ($\bar{u}(1) > 0.3$). This means almost

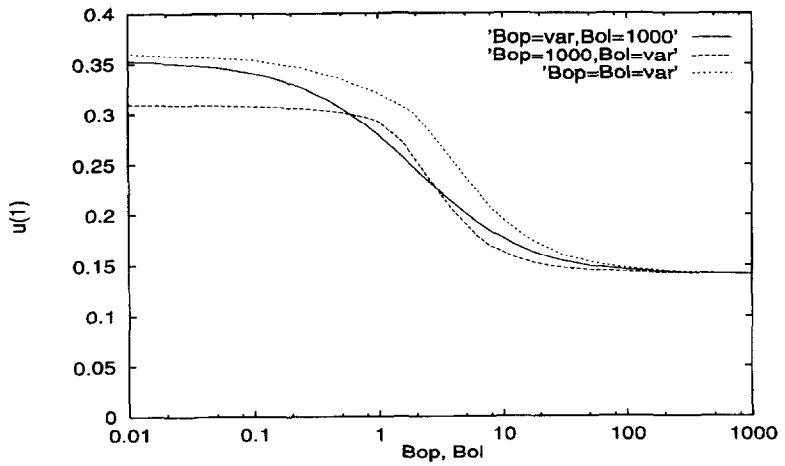


Fig. 10. Dependence of $\bar{u}(1)$ on Bo numbers.

ideal mixing, hence a simpler continuous stirred tank reactor (CSTR) model can be used. At higher *Bo* numbers (e.g. $>100$) the concentration $\bar{u}(x)$ reaches a lower end concentration ($\bar{u}(1)<0.15$), then a simpler plug flow reactor (PFR) model can be used.

## 5. Conclusions

The proposed mathematical model, based on a single particle approach and on the definition of an internal diffusivity as well as on the axial dispersion in both bulk phases, has been developed to simulate extraction of oligomers from pellet polymers in a batch extractor and in a continuous countercurrent extractor. Provided distribution equilibrium data are available, the extraction profiles can be predicted accurately. Internal resistances due to micropore diffusion or oligomer–polymer adsorption can influence the mass transfer process, in this case the balance of the polymer pellet has to be completed by an additional adsorption term.

## Appendix A. Notation

| | |
|---|---|
| $A$ | interfacial area ($cm^2$) |
| $Bo_L$ | Bodenstein number ($=lv_L/E_L$) (–) |
| $Bo_p$ | Bodenstein number ($=lv_p/E_p$) (–) |
| $c$ | concentration in the pellet (wt.%) |
| $c_0$ | starting concentration in the pellet (wt.%) |
| $c^b$ | concentration in the bulk phase (wt.%) |
| $\bar{c}$ | mean concentration in the pellet (wt.%) |
| $d$ | diameter of the extractor column (cm) |
| $D$ | diffusivity in the pellet ($cm^2\ min^{-1}$) |
| $D_L$ | diffusivity in the interface film ($cm^2\ min^{-1}$) |
| $E$ | dispersion coefficient ($cm^2\ min^{-1}$) |
| $h$ | discretization step (–) |
| $h(c)$ | distribution function (wt.%) |
| $H(u)$ | dimensionless distribution function (–) |
| $k_i$ | parameters in Eq. (16) (–) |
| $l$ | length of the extractor column (cm) |
| $n$ | total number of pellets (–) |
| $\sigma$ | dimensionless pellet residence time (–) |
| $\rho$ | dimensionless solvent residence time (–) |
| $r$ | pellet radius variable ($0<r<1$) (–) |
| $R$ | pellet radius (cm) |
| $t$ | time (min) |
| $T$ | temperature (K) |
| $u$ | concentration ($=c/c_0$) (–) |
| $u^b$ | concentration ($=c^b/c_0^b$) (–) |
| $\bar{u}$ | mean concentration (–) |
| $v$ | linear velocity ($cm\ min^{-1}$) |
| $V$ | volume ($cm^3$) |
| $V_R$ | extractor volume ($cm^3$) |
| $\bar{V}$ | volumetric flow rate ($cm^3\ min^{-1}$) |
| $x$ | axial coordinate ($0<x<1$) (–) |
| $\gamma$ | resistance number ($=D_L(1+R/\delta)/D$) (–) |
| $\delta$ | film thickness (cm) |
| $\eta$ | phase ratio ($=V_p/V_L$) (–) |
| $\tau$ | residence time (min) |

*Subscripts*

| | |
|---|---|
| f | feed |
| L | solvent phase |
| p | pellet phase |

## References

[1] BASF Company, OS Patent 1,770,097, 1968.
[2] H.B. Copelin, Method for reducing oligometric cyclic ether content of a polymerizate, US Patent 4,306,058, 1981.
[3] E.F. Barry, P. Ferioli, J.A. Hubball, Purification of OV-17 by supercritical fluid fractionation for fused silica capillary gas chromatography, J. High Res. Chrom. Chrom. Commun. 6 (1983) 719.
[4] S. Sridhar, H. Hartig, Modell zur Extraktion von Kunststoffgranulat mit Füssigkeiten, Chem. Ing. Tech. 13 (1974) 46.
[5] H.-J. Warnecke, J. Prüss, Modeling isobutene extraction from mixed $C_4$-streams, Chem. Eng. Sci. 47 (3) (1992) 533.

[6] L.M. Sun, F. Meunier, An improved finite difference method for fixed-bed multicomponent adsorption, AIChE J. 37 (1991) 244.
[7] H.Y. Wong, Heat Transfer for Engineers, Longman, Birmingham, AL, 1977, p. 36.
[8] T.L. Chen, J.T. Hsu, Predication of breakthrough curves by the application of fast Fourier transform, AIChE J. 33 (1987) 1387.
[9] Z. Chen, Ein mathematisches Modell zur Beschreibung der Tropfengrössenverteilung in dispersen Systemen, VDI, Düsseldorf, 1995.
[10] V. Pereyra, An adaptive finite-difference Fortran program for first order nonlinear, ordinary boundary problems, in: B. Childs, M. Scott, J.W. Daniel, E. Denman, P. Nelson, Codes for Boundary-Value Problems in Ordinary Differential Equations, Springer, 1979.